

# Design and Implementation of Sweeping Robot Based on SLAM

**Min Hong**

Zaozhuang University, Zaozhuang, Shandong, 266700, China

**Abstract:** The SLAM technology based on the RBPF algorithm provides key support for the intelligentization of sweeping robots, but the traditional RBPF algorithm has a slower convergence speed, and its positioning accuracy needs to be improved. Therefore, for improving the real-time performance of SLAM algorithm, it is proposed to replace the ICP algorithm with an improved radar frame data matching algorithm based on the linear expression of lidar data, at same time, in order to make the sweeping robot is more in line with the use environment and usage requirements, improved SLAM is applied to the updated design of the sweeping robots.

**Keywords:** Lidar, SLAM, Sweeping robot.

## 1. Introduction

With the continuous advancement of technology, sweeping robots have combined the advantages of traditional vacuum cleaners and autonomous mobile robots to appear on the market. The simultaneous localization and mapping(SLAM) technology provides a key support for the intelligentization of sweeping robots. The Rao-Blackwellized Particle Filters (RBPF) algorithm is the key to solving the problem of positioning and map creation[1]. However, in the traditional RBPF algorithm, the recommended distribution function of particles is determined based on the odometer reading, and the odometer has a large error. During the operation of the robot, there may be uncertain situations such as wheel slippage. Therefore, the recommended distribution of particles based on the odometer readings will slow the convergence speed of the algorithm and affect the positioning accuracy. It has been reported in the literature that an environment map construction method based on iterative closest point (ICP) algorithm and particle filter improves SLAM[2]. However, the traditional ICP matching algorithm is difficult to maintain its matching accuracy due to low computational efficiency and high computational complexity. Therefore, in order to improve the real-time performance of the improved SLAM algorithm, this design proposes an improved radar frame data matching algorithm based on the linear expression of lidar data to replace the ICP algorithm. At the same time, in order to provide support for the full arrival of the smart home era, this research applies the improved SLAM to the sweeping robot control system to make the sweeping robot more in line with the use environment and requirements.

## 2. Model construction

### 2.1 Construction of robot motion model

The robot's running model is established in two cases. In the case of linear motion, the robot's travel distance is equal to the wheel's travel distance. Assuming that the wheel does not slip during the travel, the robot's travel distance  $S$  is equal to the odometer record value  $L$ . Taking into account the certain error of the odometer, the actual situation is:

$$S = L + \varepsilon \quad (1)$$

Among them  $\varepsilon$  odometer measurement error, and the error can be regarded as Gaussian distribution.

When the robot is turning, the turning of the robot is performed by the differential speed of the driving motors distributed on both sides. The larger the differential ratio, the smaller the turning radius. Because the universal wheel only assists in running and plays the role of supporting the frame, the structure of the robot is simplified.

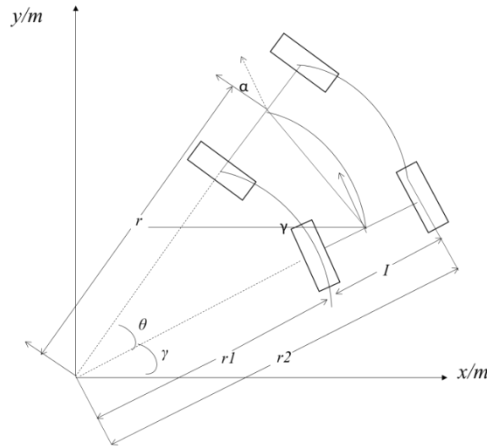


Figure 1 Simplified robot motion model

The figure shows a simplified model of the robot, where  $r_1$ ,  $r_2$  are the turning radius of the left and right wheels,  $r$  is the turning radius of the geometric center of the robot,  $l$  is the installation distance of the left and right wheels, and  $l_1$  and  $l_2$  are the distances of the left and right wheels. It is assumed here that the robot wheel is not slipping, and this value is the value recorded by the odometer.  $\alpha$  is the change of the heading angle of the robot,  $\theta$  is the turning angle of the robot, and  $\gamma$  is the X-axis angle between the robot's initial pose and the world coordinate. The figure shows:

$$r_2 = r_1 + 1 \quad (2)$$

The robot makes a turning motion around a fixed point, and calculates the stroke of the left and right wheels.

$$\begin{cases} l_1 = r_1 \times \theta \\ l_2 = r_2 \times \theta \end{cases} \quad (3)$$

Assuming that the initial pose of the robot is as shown in the figure, the initial pose is  $(x_1, y_2, \gamma)$ , then the pose of the robot after turning  $(x, y, \lambda)$

$$\begin{cases} x = x_1 + 2 \cdot r \cdot \sin\left(\frac{\theta}{2}\right) \cos\left(\frac{180-\theta}{2} - \gamma\right) = x_1 + 2r \cdot \sin\left(\frac{l_2-l_1}{2l}\right) \cdot \sin\left(\frac{l_2-l_1}{2l} + \gamma\right) \\ y = y_1 + 2 \cdot r \cdot \sin\left(\frac{\theta}{2}\right) \sin\left(\frac{180-\theta}{2} - \gamma\right) = y_1 + 2r \cdot \sin\left(\frac{l_2-l_1}{2l}\right) \cdot \cos\left(\frac{l_2-l_1}{2l} + \gamma\right) \\ \lambda = \gamma + \theta = \gamma + \frac{l_2-l_1}{l} \end{cases} \quad (4)$$

As shown above, the robot's motion model based on the odometer can calculate the position and posture changes of the robot according to the odometer information. The operation control of the actual robot also needs to control the rotation speed of the left and right wheels to make the robot perform a turning movement with a certain turning radius and angular velocity. The following discusses the rotation speed control of the left and right wheels under the conditions of a specified turning radius of  $r$  and an angular velocity of  $\omega$ .

$$\begin{cases} r_1 = r - \frac{l}{2} \\ r_2 = r + \frac{l}{2} \end{cases} \quad (5)$$

If the turning radius of the robot is known, the turning radius of the left and right wheels can be obtained. If the angular velocity is  $\omega$ , the rotation speed of the left and right wheels can be calculated as:

$$\begin{cases} v_1 = \omega \cdot r_1 = \omega \cdot \left(r - \frac{l}{2}\right) \\ v_2 = \omega \cdot r_2 = \omega \cdot \left(r + \frac{l}{2}\right) \end{cases} \quad (6)$$

## 2.2 Map model construction

This study uses the grid map method to construct an environmental map[3].The state of a grid is represented by 0 and 1. 1 means that the grid is in an occupied state, and 0 means that the grid is in an

idle state. In addition,  $p(m_{x,y}=1)$  indicates the probability that the grid is in an occupied state,  $p(m_{x,y}=0)$  indicates the probability that the grid is in an idle state, and subscript  $x y$  to indicate the grid position. The measurement status is represented by  $z$ ,  $z=1$  means the grid measurement result is occupied,  $z=0$  means the grid measurement result is idle. Additionally, the odds (odd) expression method is used to express the ratio of the probability of occurrence and non-occurrence at a time,

$$\text{odd} : \frac{P(\text{Xhappens})}{P(\text{Xnothanppens})} = \frac{p(X)}{p(X^c)} \quad (7)$$

According to Bayes' rule[4]:

$$p(m_{x,y} = 1 | z) = \frac{p(z|m_{x,y}=1)p(m_{x,y}=1)}{p(z)} \quad (8)$$

$$p(m_{x,y} = 0 | z) = \frac{p(z|m_{x,y}=0)p(m_{x,y}=0)}{p(z)} \quad (9)$$

In order to facilitate the calculation, the logarithmic transformation of the above formula is carried out,

$$\log \text{odd}(m_{x,y} = 1 | z) = \log \frac{p(z|m_{x,y}=1)}{p(z|m_{x,y}=0)} + \log \frac{p(m_{x,y}=1)}{p(m_{x,y}=0)} \quad (10)$$

$\log \text{odd}^+(\text{posteriori probability})$

$$= \log \text{odd means}(\text{likelihood estimation}) + \log \text{odd}(\text{prior probability}) \quad (11)$$

According to the above calculation, the posterior value can be obtained by adding and subtracting the prior value and the likelihood value. The higher the log-occupied win rate, the higher the probability of possession of the grid, on the contrary, the lower the log-occupied win rate, the higher the probability of being idle.

### 3. Lidar data processing

#### 3.1 Lidar drive and data extraction

The lidar used in this research is the EAI-X4 lidar produced by EAI Technology Company. The control platform of the robot is Raspberry Pi, the ROS system is installed in the Raspberry Pi[5].The lidar is connected to the Raspberry Pi through a data cable to realize power supply and communication to the lidar.The lidar data format under the subject of /scan is as follows:

```
header:
seq: 5925
stamp:
secs: 1532266695
nsecs: 102719943
frame_id: laser frame
angle_min: - 3.14159274101
angle_max: 3.14159274101
angle_increment: 0.00872664819237
time_increment: 0.000210903861444
scan_time: 0.151850774884
range_min: 0.0799999982119
range_max: 10.0
ranges: [0.0,0.0,0.0,2.494999885559082,
2.7320001125335693,2.746000051498413,0.0,0.
3.0280001163482666,3.0280001163482666,3.0120
```

#### 3.2 Removal of invalid points and coordinate conversion

Due to the sensor errors or radar losing data during fast scanning,the data obtained directly from the lidar is flawed, There are some discrete points and invalid points in the obtained data. These invalid points will seriously affect the measurement accuracy and increase the amount of invalid calculations, which will cause unnecessary trouble for the subsequent robot positioning and map construction.

Therefore, the data needs to be processed in the early stage. Data processing is mainly divided into two parts, one is to remove invalid data points and carry out coordinate conversion, and the other is to identify feature points and remove discrete points. The EAI-X4 radar has 720 data in each frame of data, corresponding to 720 measurement angles evenly distributed in a circle of 360 degrees.

A frame of point cloud data obtained from the radar is recorded as:

$$A = \{\rho_i, v_i | i = 1, 2, 3, \dots, N\} \quad (12)$$

In the formula:  $\rho_i$  represents the distance from the obstacle detected at the  $i$ -th point to the lidar;  $v_i$  represents the angle between the scanning direction of the  $i$ -th point and the radar direction.

The point cloud data is expressed in polar coordinates. In order to facilitate processing, the radar data is converted to a rectangular coordinate system:

$$\begin{aligned} x_i &= \rho_i \times \cos(v_i) \\ y_i &= \rho_i \times \sin(v_i) \\ A &= \{\alpha_i = (x_i, y_i) | i = 1, 2, 3, \dots, N\} \end{aligned} \quad (13)$$

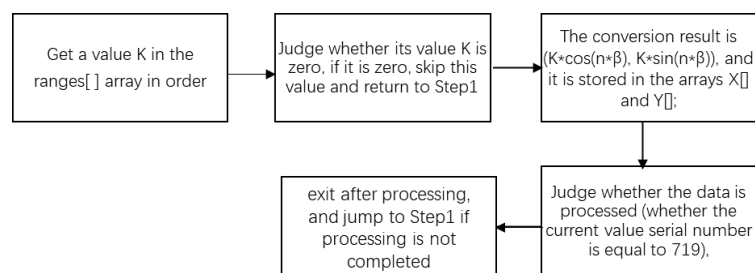


Figure 2: Coordinate transformation algorithm flow chart

### 3.3 Feature extraction

Because the indoor environment is layered and scattered, the place scanned by the laser is not a continuous plane, and the data obtained is therefore gathered in sections. Each piece of data corresponds to a scanning surface and has corresponding characteristics. For processing radar data, it is necessary to segment the data. The data segmentation method used in this paper is an improvement based on the Euclidean distance method, and its threshold is set to an adaptive size.

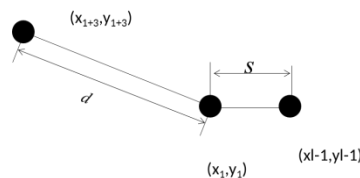


Figure 3: Improved segmentation algorithm

$$\Delta_i > \varepsilon \parallel \frac{\max(\Delta_i, \Delta_{i-1})}{\min(\Delta_i, \Delta_{i-1})} > \tau \quad (14)$$

Among them,  $\Delta_i$  is the distance between  $p_i$  point and  $p_{i+1}$  point, and  $\Delta_{i-1}$  is the distance between  $p_i$  point and  $p_{i-1}$ .  $\varepsilon$  is the distance threshold,  $\tau$  is the ratio threshold.

## 4. Improved matching algorithm based on SLAM

### 4.1 ICP algorithm improvement

In order to facilitate the algorithm design and calculation, the search for the transfer matrix is divided into two parts. First, the rotation angle is determined, and then the translation amount is determined.

Sort the class set according to the record length  $l_i$ , and take the first two classes as the main orientation of the indoor environment. Extract the main orientation from the point cloud of the two

frames A and B, and record it as:  $\lambda_A = (\lambda_{A1}, \lambda_{A2}), \lambda_B = (\lambda_{B1}, \lambda_{B2})$  .

If the orientation order is correct, the difference between the corresponding orientation angles should be similar. If not, the order will be reversed. Adjust the main orientation order of the A-frame point cloud. Use the obtained main orientation information to perform initial rotation matching on the point cloud, and obtain the rotation angle as:

$$\theta'_{A,1} = \frac{1}{2}((\lambda_{A1} - \lambda_{B1}) + (\lambda_{A2} - \lambda_{B2})) \quad (15)$$

After obtaining the main direction, it is updated as the point cloud data:

$$B' = \begin{pmatrix} \cos(\beta - \alpha) & -\sin(\beta - \alpha) \\ \sin(\beta - \alpha) & \cos(\beta - \alpha) \end{pmatrix} \cdot B \quad (16)$$

Where  $\beta$  is the main direction angle of the target point cloud, and  $\alpha$  is the main direction angle of the point cloud to be matched. After preliminary matching, the two frames of point cloud data are basically parallel.

The calculation steps of the translation amount are as follows:

Step1: Select a corner point  $j_{Bi}$  in the point cloud to be matched, and match it with the corner point  $j_{Ai}$  in the target point cloud in turn;

Step2: If the matching is successful, record the distance difference  $t_i(\Delta x_i, \Delta y_i)$  between the matching corner points. If the matching fails, select the next corner point  $j_{Bi+1}$  from the point cloud to be matched and continue matching;

Step3: Complete the matching, obtain the distance difference between the matching corner points  $(t_1, t_2, t_3, \dots)$ , and obtain the optimal value by the least square method as the translation amount  $t(\Delta x, \Delta y)$ .

#### 4.2 Improved RBPF algorithm combining matching algorithms

In order to improve the reliability of the algorithm and avoid the failure of the SLAM algorithm due to errors in lidar data matching, Therefore, it is necessary to judge the result of lidar data matching first. When the matching result meets the requirements, the lidar matching result is selected as the recommended distribution function of particles, and when the matching result has obvious errors, the odometer data is selected as the recommended distribution function.

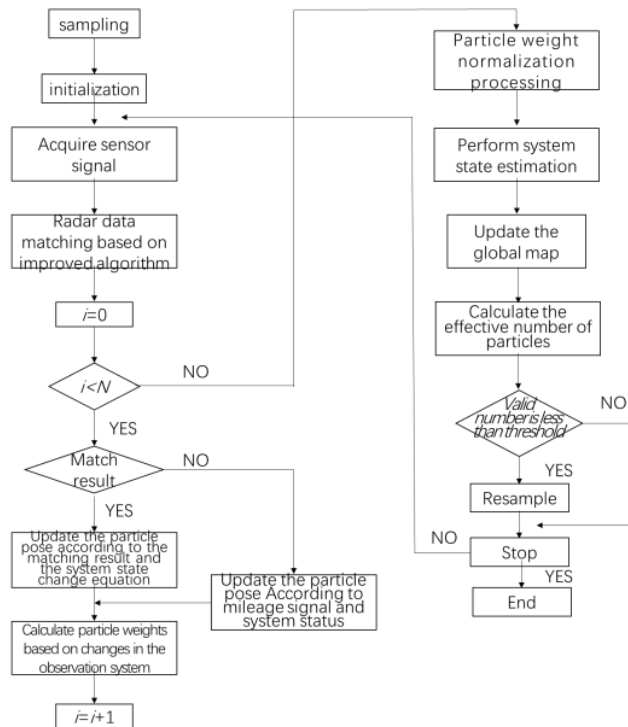


Figure 4: Flow chat of improved algorithm

## 5. Design and implementation of the sweeping robot control system

This article chooses to mount the control system on the Klinsmann sweeping robot site, complete the installation and debugging of the control system, and build a hardware experiment platform.

The wheel position relationship of the chassis of the sweeping robot is shown in Figure 4, where wheels A and B are left and right wheels driven by a DC motor, and wheel C is a universal wheel without a power source. After actual measurement, the diameter  $D_{AB}$  of wheels A and B is 0.07m, and the thickness is 0.015m. The diameter of universal wheel C is 0.014m, and the thickness is 0.01m. The wheel center distance  $l_{AB}$  between the left and right wheels A and B is 0.22m, and the distance  $l_{OC}$  of the universal wheel to the center of the vehicle body is 0.11m.

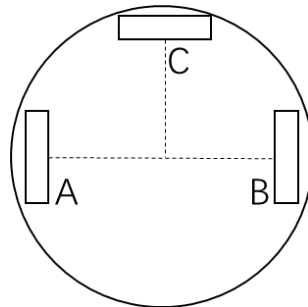


Figure 5: Schematic diagram of wheel distribution

After completing the selection and related calculation of each module of the sweeping robot control system, the installation, connection and debugging of each module can be carried out. This article uses DuPont cable, USB cable, CSI cable and other modules to connect to the control system. The specific hardware wiring diagram is shown in Figure 6.

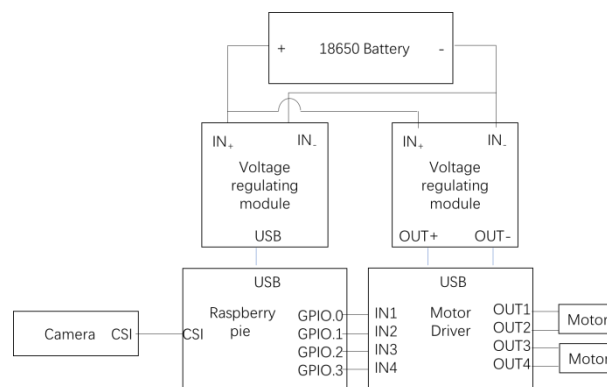


Figure 6: Schematic diagram of hardware wiring

## References

- [1] Dai X, Sun X, He J, et al. Improved Grid-Based Rao-Blackwellized Particle Filter SLAM Based on Grey Wolf Optimizer[J]. JOURNAL OF BEIJING INSTITUTE OF TECHNOLOGY, 2021, 30(zk):23-34.
- [2] Min Z. A Multi-view Point Clouds Registration Method Based on ICP Algorithm[J]. Sci-tech Innovation and Productivity, 2017.
- [3] Zeyu, Tian C, Guo Y, et al. An Improved RRT Robot Autonomous Exploration and SLAM Construction Method[C]// 2020.
- [4] Yu R. A Tutorial on VAEs: From Bayes' Rule to Lossless Compression[J]. 2020.
- [5] Vanicek P, Beran L. NAVIGATION OF ROBOTICS PLATFORM IN UNKNOWN SPACES USING LIDAR, RASPBERRY PI AND HECTOR SLAM. 2018.